AN ABSTRACT OF THE THESIS OF

WILLIAM HAROLD GUMMA (Name of student) for the MASTER OF SCIENCE (Degree)

in OCEANOGRAPHY (Major) presented on September 7, 1973 (Date)

Title: AN INTERPRETATION OF THE GRAVITY AND MAGNETIC ANOMALIES OF THE RIVERA FRACTURE ZONE, EASTERN PACIFIC OCEAN

Redacted for privacy

Abstract approved: Richard W. Couch

Gravity data, collected during a ten day survey of the Rivera fracture zone and combined with existing refraction information to construct crustal and subcrustal cross sections, reveals that the Rivera fracture zone is underlain by a compensating root of low density. Along portions of the fracture zone which are topographically well-defined, layers with postulated densities of 2.61 and 2.84 gr/cm^3, normally associated with oceanic layers II and III respectively, appear to outcrop in the walls of the central trough. Beneath the central trough of the fracture zone, the 2.61 gr/cm^3 layer usually 1 km thick, increases to a thickness of 3 km over a 10 km wide area. The crust-mantle interface, which is usually at a depth of 8-9 km, begins to increase in depth 20-30 km from the fracture and reaches a maximum depth of 14-15 km directly beneath

the central trough. In areas where the fracture zone is not topographically distinct, widely separated areas of slightly thickened 2.61 gr/cm^3 material are underlain by a 10-11 km deep crust-mantle interface.

Theoretical magnetic anomaly profiles constructed using simple magnetic models along with the observed topography indicate that the sources of the observed magnetic anomalies are remnant fields associated with layer II basalts. These source bodies, which may originate at mid-ocean rises, are physically or magnetically discontinuous across the fracture zone.

Fault brecciation and hydrothermal alteration are the postulated causes of the expunged magnetics and low density sections. Geometrical considerations and uplift, caused by the expansion of altered mantle material, provide a simple explanation for the origin of fracture zone topography.

An Interpretation of the Gravity and Magnetic Anomalies of the Rivera Fracture Zone, Eastern Pacific Ocean

by

William Harold Gumma

A THESIS

submitted to

Oregon State University

in partial fulfillment of
the requirements for the
degree of

Master of Science

Commencement June 1974

APPROVED:

Redacted for privacy

Assistant Professor of Geophysics
in charge of major

Redacted for privacy

Dean of the School of Oceanography

Redacted for privacy

Dean of the Graduate School

Date thesis is presented September 7, 1973

Typed by Chris Pastega for William Harold Gumma

ACKNOWLEDGEMENTS

This research was guided by Dr. Richard W. Couch. I am grateful to him for his encouragement and advice during the past two years.

I am also grateful to Michael Gemperle, Ken Keeling, Gordon Ness and Vic Rosato for their help and suggestions during data preparation and analysis, and to Janet Gemperle for drafting the figures used in this text.

Drs. William P. Elliot and Stephen Johnson reviewed this thesis and made helpful suggestions.

This research was supported by the Office of Naval Research, contract N00014-67-A-0369-0007 under project NR 083-102.

TABLE OF CONTENTS

LIST OF FIGURES

LIST OF TABLES

AN INTERPRETATION OF THE GRAVITY AND MAGNETIC ANOMALIES OF THE RIVERA FRACTURE ZONE, EASTERN PACIFIC OCEAN

INTRODUCTION

In April, 1972, personnel of the Geophysics Group of Oregon State University surveyed the Rivera fracture zone, a seismically active 400 km long offset in the East Pacific Rise system off Acapulco, Mexico. A ten day survey was designed to study the crustal and subcrustal structure of a young fracture zone and to determine, if possible, the nature of the tectonic forces involved in creating these unique features of the ocean floors.

Menard and Dietz (1952) described the Mendocino fracture zone in the eastern Pacific Ocean in 1952, and in the years following, researchers located many more (e.g. Menard, 1964). Fracture zones are usually bathymetrically distinct from the surrounding sea floor because of their high relief and extreme linearity. Some of the eastern Pacific fracture zones are over 2000 km long, certainly marking them as the most conspicious features on earth.

With the introduction of the transform fault by Tuzo Wilson (1965) and the evolution of the plate tectonic theories of the late 1960's (e.g. Morgan, 1968, Isacks et al., 1968), fracture zones received considerably more attention. Their orientation became an important geometric tool which helped to indicate the complex

motions involved in the creation, motion and subduction of large rigid plates on a spherical earth.

Today, fracture zones are not only defined bathymetrically, but also by offsets in magnetic anomaly patterns produced by mid-ocean ridges and by linear bands of seismicity. Despite the implications drawn from fracture zone orientation by nearly all geological and geophysical investigators involved with plate tectonics, fracture zones are poorly understood as a physical phenomena. Their structure and the role they play in global tectonics, whether passive or active, is largely unknown.

PREVIOUS WORK

Topography of Fracture Zones

The most common topographic feature of fracture zones besides high relief and extreme linearity, is the presence of a central trough, usually deeper than the adjacent sea floor and surrounded by high standing parallel ridge systems. Most studies to date have been concerned with surveying this topography along with the surrounding mid-ocean ridge system for the purpose of defining the present tectonic situation of a specific area. Several investigators expanded these studies and developed partial geometrical and dynamic explanations for fracture zone topography. van Andel, et al. (1968, 1971) in an extensive study of the Vema fracture zone of the central Atlantic, proposed that as a result of a reorientation in spreading direction, the fracture zone itself is the site of secondary spreading. They suggested that spreading takes place by the injection of thin dikes into the fracture zone walls.

Menard and Atwater (1969) first proposed this general concept. They developed a simple geometrical model which explained general elevation differences observed across some fracture zones. They further observed that the elevation of mid-ocean ridges is roughly inversely proportional to the spreading rate, and concluded that

fracture zone topography must be a direct result of an extremely small component of spreading normal to transform faults. The work of Sleep and Biehler (1971) gave some credibility to this rather circular argument. They invoked viscous drag forces and resulting head loss in magma upwelling at fracture zone-rift intersections in order to explain the observed central trough. The fact that the deepest portion of many fracture zones is at the fracture-ridge intersection supports this model. Uplift, associated with recovery of lost head as the topography spreads away from the ridge, may account for the raised fracture zone walls (Sleep, 1969).

These models seem to fit the equatorial Atlantic fracture zones fairly well. However, their applicability to all types of fracture zones found in the world oceans is questionable. The differences in the character of the Atlantic and Pacific mid-ocean ridge systems suggest that fracture zones may also be expected to vary from one region to another. Still, one would expect to find some basic dynamic model which would apply to all fracture zones.

To a large degree, the models of Sleep and Biehler (1971) and Menard and Atwater (1969) depend upon a recent reorientation in spreading direction. It is difficult to envision all fracture zones as leaky. Further complications arise when one considers the fact that fracture zone topography does not exist along whole segments of many fractures, especially in the Pacific Ocean. Also unexplained by the fracture-

ridge intersection models is how fracture zone topography can exist along portions of oceanic crust which was not the product of fracture-ridge intersection areas. This situation arises in particular among Pacific fracture zones which are relatively young and which exhibit large ridge offsets.

The implication is that fracture zone topography, to a certain degree, is independent of ridge-fracture zone intersections and spreading direction changes.

Petrology of Fracture Zones

Because of their rugged topography, fracture zones provide excellent locations for dredging the mid-ocean rise systems, and much of the petrologic data concerning fracture zones is obtained in studies of mid-ocean rises. Matthews et al. (1965), Melson and Thompson (1971), Aumento and Lubat (1971), Bonatti et al. (1970) and many other investigators report dredging nearly every type of oceanic rock known or postulated to exist from fracture zone scarps. This has generally led to many complications in the speculative explanations of fracture zone dynamics, for any acceptable model must account for this cornucopia of varied petrology.

Probably the most comprehensive paper in this field is that of Thompson and Melson (1972). After an in-depth analysis of several Atlantic fracture zones, they concluded that fracture zones are sites

of basic rock extrusions and intrusions as well as intrusions of ultra-basic plutonic rock believed to be of upper mantle origin. It is further suggested that oceanic crust is created along the fracture zone and that this crust differs chemically from the crust created at ridge crests.

Gravity Observations Over Fracture Zones

A sizeable amount of geophysical data already exists over the regions of the ocean floors where fracture zones are most abundant. However, most gravity and magnetic data available comes from surveys of adjacent features, such as mid-ocean ridges, and is not well suited for fracture zone analysis. Only a few gravity studies of fracture zones are available. One, by Dehlinger, et al. (1967) is a survey of the Mendocino escarpment, a mostly relic fracture zone. Their refraction and gravity constrained crustal sections indicate that the Mendocino escarpment is mirrored by an escarpment in the earth's mantle and that the fracture zone separates regions of different mantle densities.

Cochran (1973), in a composite gravity survey of several equatorial Atlantic fracture zones concluded that they are the locations of local mass excess. In order to account for the observed free-air anomaly it was necessary to introduce additional mass beneath the fracture zone trough and ridges. Two alternate theories are

offered to explain the observed data. Thompson and Melson (1972) suggested that fracture zones are sites of large scale intrusions of serpentine. Serpentine, which is a low temperature hydration product of olivine, varies considerably in density as a function of the degree of alteration. It is possible that these intrusions may appear as local mass excesses when contrasted against light material of the type associated with layer II.

An alternate explanation is that fracture zones are essentially windows into the lower oceanic crust. This view is supported by dredge hauls which have produced samples of basic and ultrabasic rocks from fracture zone scarps. Layer III is postulated to be a mixture of various basic and ultrabasic plutonic rocks (Melson and Thompson, 1970, 1971). These layers, void of the usual upper crustal material, might also appear as mass excesses. Cochran sees fracture zones as the sites of extensive serpentine intrusions, but concedes that basaltic rocks must also be present.

Magnetic Anomalies Over Fracture Zones

Fracture zones are well known for their distinct magnetic anomaly patterns. The amplitude of the anomaly may vary, but in general, it is distinct from the adjacent sea floor spreading anomalies (Rea, 1972). For many years, the concensus has been that there is a sharp positive magnetic peak situated directly over the

fracture zone trough. Cochran reported this phenomenon in his study of Atlantic fracture zones. Early speculation was that this anomaly was due to serpentine intrusions (Vogt, 1971) or basaltic accumulation in the fracture zone trough (Morgan, 1969). Cochran concluded that the observed magnetic anomaly is produced by induced magnetic sources in slabs separated by 20 km across the fracture zone. van Andel et al. (1973), in a study of the Ascension fracture zone, favor the existence of magnetic bodies parallel to the strike of the fault. They base their conclusion on correlation of several magnetic profiles taken perpendicular to the strike of the fracture zone.

To date, most studies involve a qualitative analysis of large amounts of magnetic data. Surprisingly, few people take into account the effects of topography when analyzing magnetics. The abundance of possible magnetic models may be a product of this fact and the inherent nonuniqueness of magnetic modeling in general.

GEOGRAPHICAL AND TECTONIC SETTING OF THE RIVERA FRACTURE ZONE

The Rivera fracture zone lies at 19°N, 105°W forming the western border of the Rivera lithospheric plate. This plate is separated from the Pacific lithospheric plate on the east by the East Pacific Rise, and from the American lithospheric plate on the west by the Middle America trench. To the north, the East Pacific Rise breaks up into a series of short spreading centers and en echelon faults which eventually lead into the San Andreas fault system. In the extreme southeast portion of the Rivera plate, the fracture zone forms the border between the Rivera and Cocos plates (Figure 1).

The interpretation of magnetic anomalies (Larson, 1972) indicates that the Rivera fracture zone and corresponding plate came into existence somewhere between 4 and 10 million years ago following a general reorientation of the East Pacific Rise system south of the mouth of the Gulf of California. Recently, some controversy exists as to whether the Rivera plate is an independent plate actively underthrusting the North American plate, or attached to and part of the larger North American plate. (Larson (1972) favored the latter view based on parallelism between the Rivera fracture zone and en echelon faults in the Gulf of California. However, Molnar (1973) determined focal mechanisms for eight earthquakes on the Rivera fracture zone and found that the direction of motion was not the same as that expected

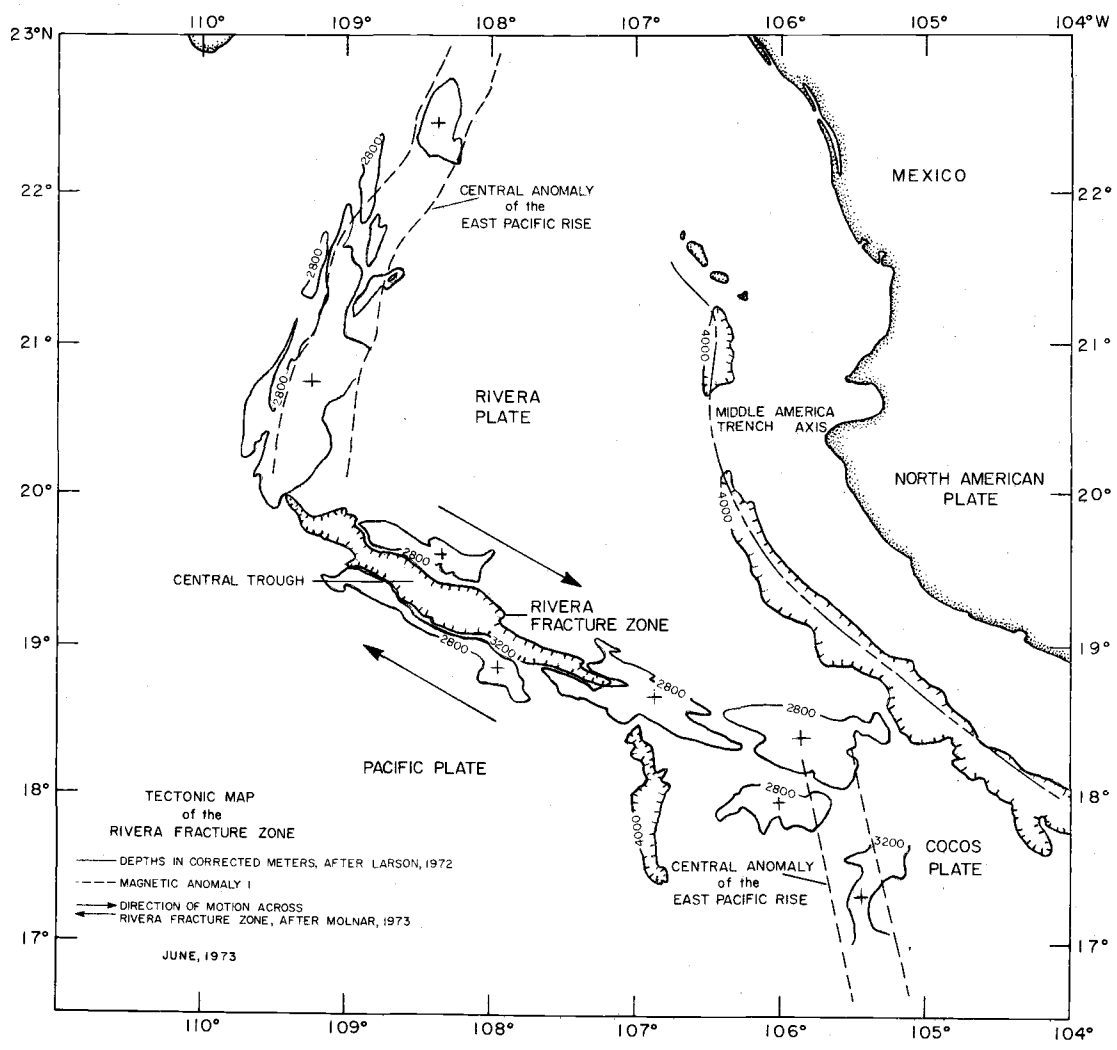

Figure 1. Tectonic map of the Rivera fracture zone area.

for a Pacific-North American plate boundary. He concluded, therefore, that the Rivera plate is an independent plate.

Assuming that Molnar is correct, the Rivera plate must be presently underthrusting the North American plate in the vicinity of the Middle America trench. Larson (1972), using magnetic anomalies, estimated a half rate of approximately 3.0 cm/yr.

Physical Description of the Rivera Fracture Zone

For purposes of description the topography of the 400 km long fracture zone is divided into two parts. The western half extends from the eastern portion of the East Pacific Rise at 110°W longitude, to a north-south trending valley at 107°W longitude. This portion of the fracture zone exhibits striking fracture zone topography. A central trough at depths of 5000 meters is bordered by two high standing ridge systems, one on the south, and one on the north. The topographic relief on this portion of the fracture zone changes as much as 5.6 km vertically along a 28 km traverse (Figure 2).

The eastern half of the fracture zone, from 107°W to the Middle America trench at 105°W longitude, exhibits entirely different topography. The striking fracture zone topography gives way to low lying ridges and slight depressions of limited linear extent. The only discernable trend is an almost east-west lying series of short ridges and depressions as indicated by the 2800 meter contour

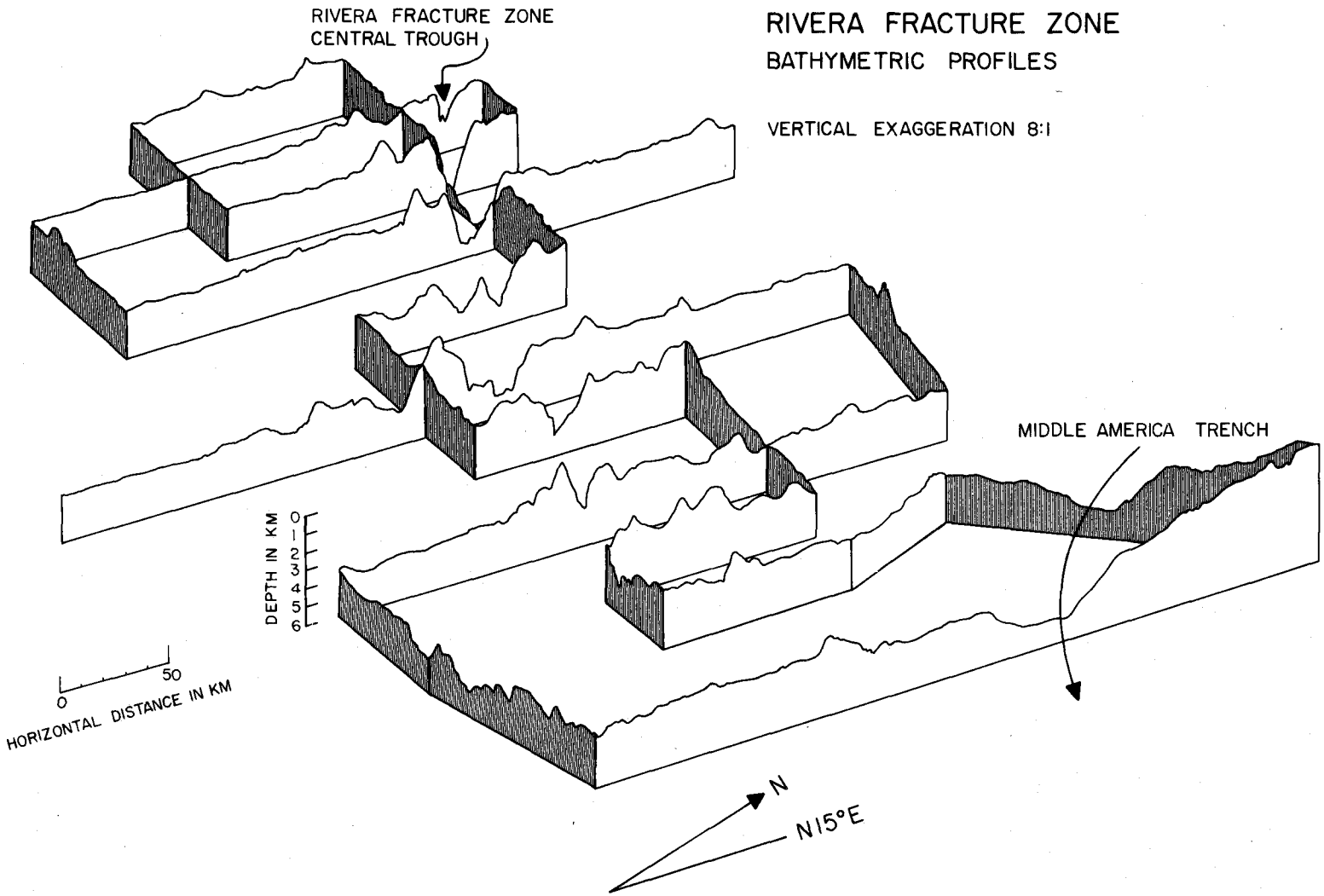

Figure 2. Bathymetric profiles from the YALOC 71 survey of the Rivera fracture zone.

in Figure 1. There is no visible continuation of fracture zone topography in this area.

Earthquake Strain Release and Focal Mechanisms

Figure 3 depicts strain release expressed in terms of equivalent body wave magnitude, earthquake epicenters and available focal mechanism solutions (Sykes, 1967, 1968 and Molnar, 1973). The offset portions of the East Pacific Rise appear as north-south trending zones of moderate strain release. The western portion of the Rivera fracture zone appears as a concentrated zone of strain release and epicenters some 50 km in width. Focal mechanism solutions show consistent right lateral motion along fractures which strike N108^{o}E.

The eastern portion of the fracture zone generally exhibits a more diffuse strain energy pattern and a more widely scattered epicenter zone. The only focal mechanism in this portion of the fracture zone indicates that the direction of strike-slip motion in this area is along fractures oriented more east-west, possibly reflecting a Rivera-Cocos plate interaction.

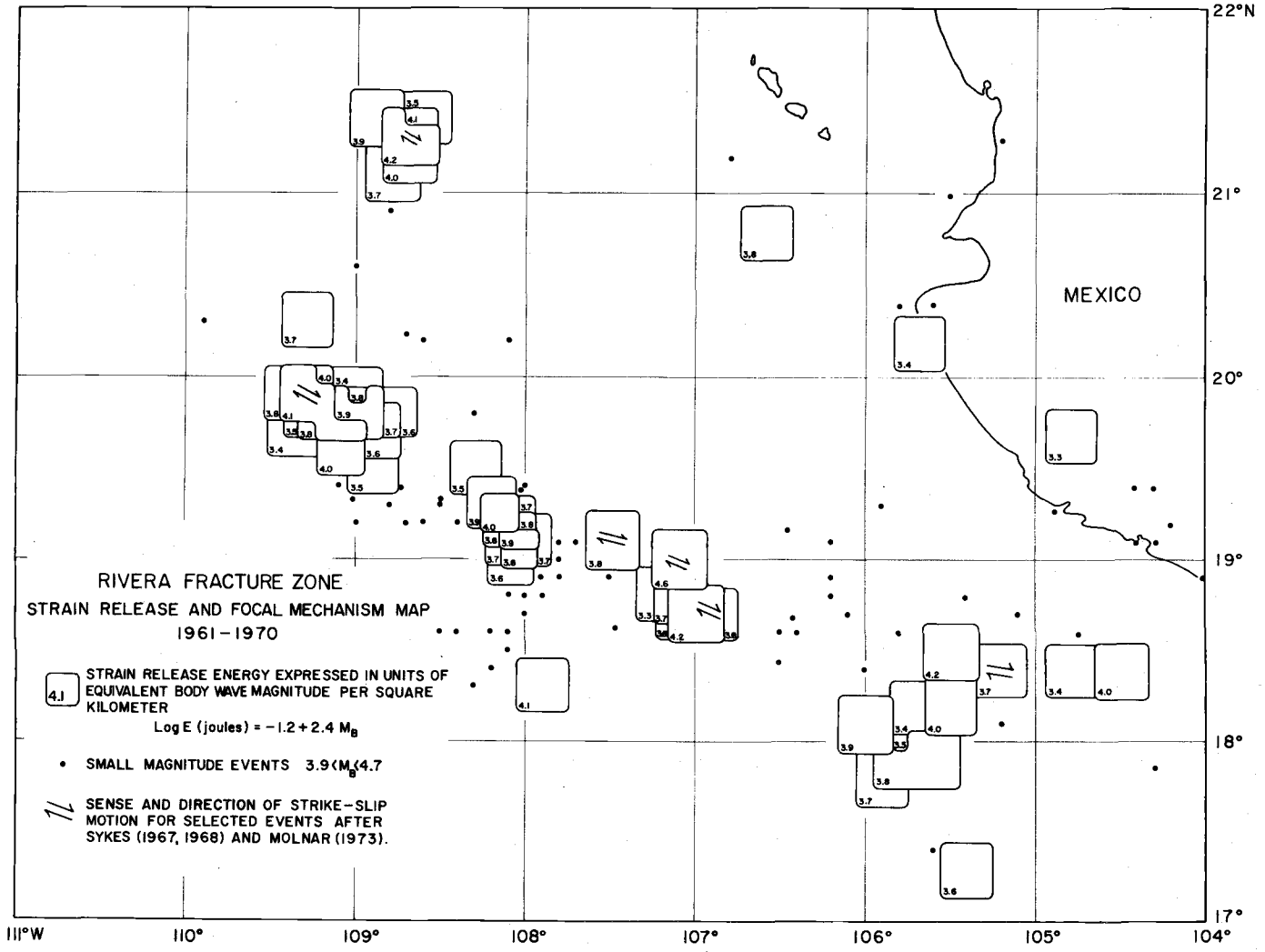

Figure 3. Earthquake strain release and focal mechanism solutions on the Rivera fracture zone.

DATA INTERPRETATION

Gravity Data

Gravity measurements were taken aboard the R/V Yaquina during a 27 day cruise in April, 1973, with LaCoste-Romberg surface ship gravity meter S-42. The meter operated on a stable-table on which accelerometers measured horizontal accelerations and an analog computer calculated cross-coupling corrections. During on-land data reduction, correlation coefficients between gravity and acceleration parameters were calculated by a matrix inversion technique and applied to the gravity measurements to correct for non-linear response of the meter caused by large ship accelerations. Final gravity values reported at five minute intervals, correspond to an average spatial frequency of 0.66 points per km.

Satellite fixes, obtained at intervals of less than two hours, provided the basis for ships navigation. Computer analysis, navigational data, including satellite fixes and ship's speed and course data, produced the final ship's trackline. Estimated navigational accuracies are $\pm$ .1 kts in ship speed, $\pm 1^{o}$ in heading and $\pm$ 0.2 km in ship position. The difference in gravity measurements at trackline crossings provides an estimate of the accuracy of the gravity meter. Of the six crossings, all but one agreed within $\pm$ 3.5 mgals. The

sixth crossing is over a small portion of the survey during which gravity meter corrections were not properly recorded on magnetic tape. The effect of cross-coupling was the only correction made to this data and the observed difference in the gravity measurements at this crossing was 12 mgals. In addition to the six internal crossings, two traverses made in 1972 crossed traverses made in 1969 with LaCoste-Romberg gimbal mounted meter S-9, aboard the R/V Yaquina. They agree with an accuracy of $\pm$ 3 mgals.

An absolute gravity value of 978,524.5 mgals measured at the monument of "A Los Heros, Febrero De 1949" in Acapulco, Mexico, provides the base tie for the survey. The accuracy between this gravity value and that measured on the ship was estimated to be $\pm$ 1.0 mgal.

Overall, the gravity data used in constructing the free-air anomaly map and structural sections reflects an rms accuracy of $\pm$ 3.6 mgals. Figure 4 shows the location of the ship tracklines and submarine pendulum stations used for construction of the free-air map.

Free-Air Gravity Anomaly Map

The most prominant feature of the free-air gravity anomaly map of the Rivera fracture zone area is the presence of a large elongate negative anomaly over the central fracture zone trough (Figure 5).

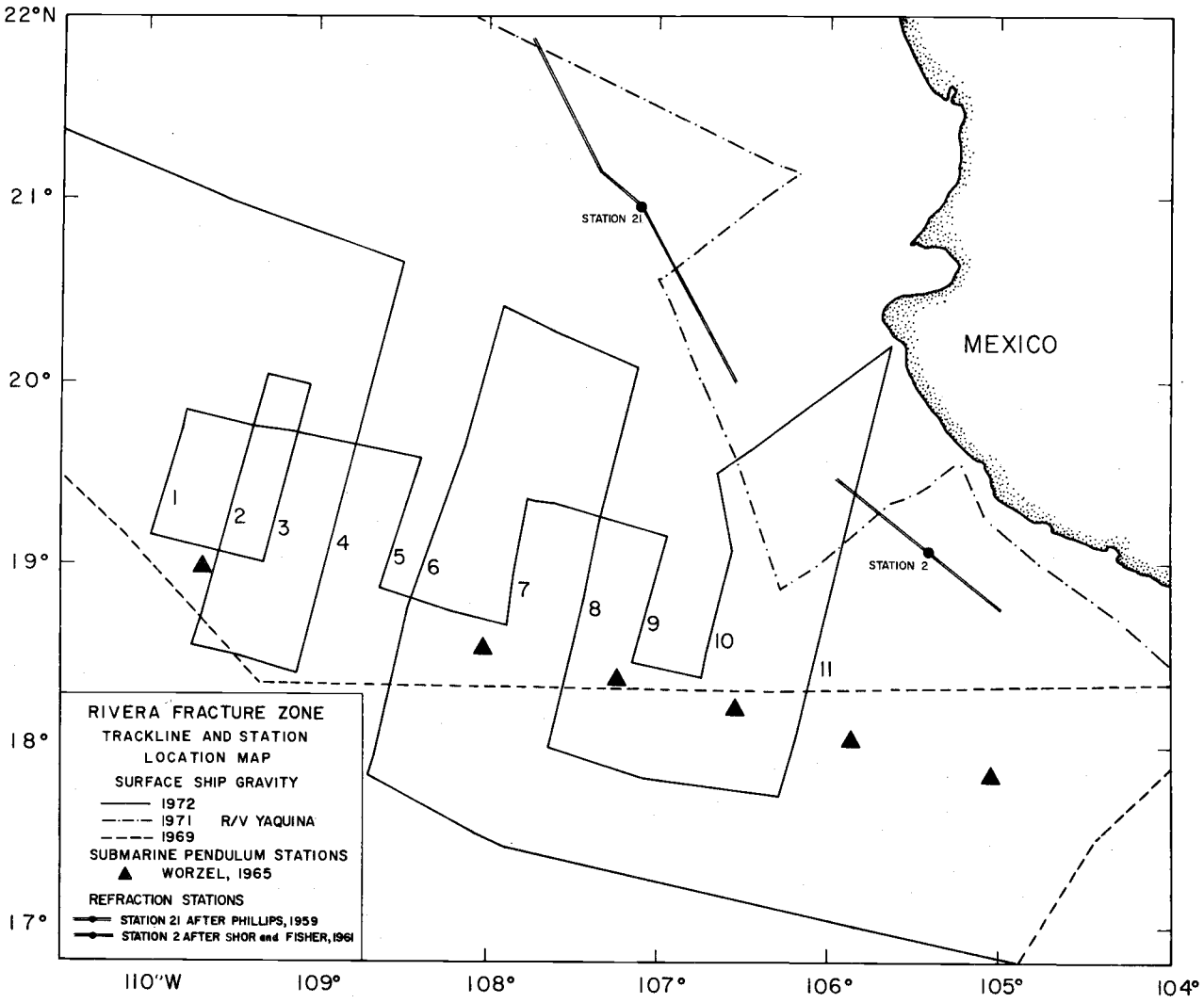

Figure 4. Index map showing location of gravity tracklines, submarine pendulum stations and refraction lines.

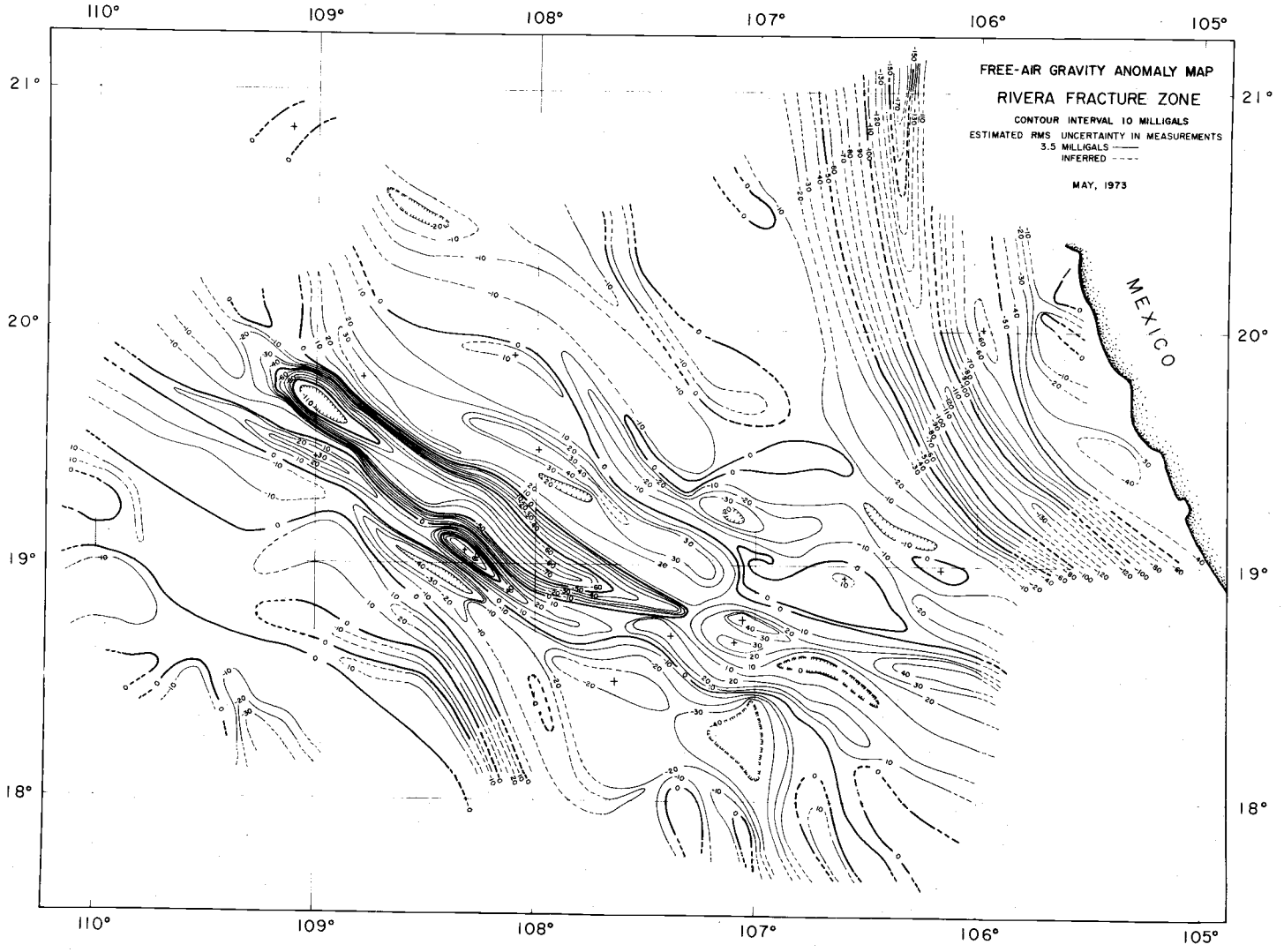

Figure 5. Free-air gravity anomaly map of the Rivera fracture zone.

Maximum negative anomalies of -120 mgals are observed in the extreme western portion of the fracture zone. This large negative anomaly is bordered on the south by a linear trend of positive anomalies corresponding to the southern ridge systems.

The north-south trending valley at 107°W longitude which topographically divides the fracture zone, exhibits negative anomalies as low as -40 mgals. East of this feature, the character of the gravity anomalies change. In contrast to the linear negative anomaly of the western fracture zone, the eastern portion exhibits mostly positive anomalies with a maximum of +48 mgal and a minimum of -30 mgal. These anomalies, although not as linear as their western counterparts, appear to strike more westerly, thus indicating that surface and possible subsurface trends change in this area.

The northeast portion of the free-air map shows prominent gravity anomalies associated with the Middle America trench. Free-air anomalies of approximately -170 mgals are colinear with the bathymetric axis of the trench.

With the exception of the trench area, the region of the Rivera fracture zone appears to be in general isostatic equilibrium, as indicated by a near zero free-air gravity anomaly for most of the surrounding region. This implies that there are no large mass imbalances indicative of driving forces associated with the general region of the fraction zone.

Crustal and Subcrustal Cross Sections

Direct knowledge of the structure of the crust and upper mantle in the area of the Rivera fracture zone comes from two large refraction studies; one by Phillips (1964) in the Gulf of California and the second by Shor and Fisher (1961) over the Middle America trench. One refraction station from each study is located close enough to the fracture zone so that it could be used as control for constructing crustal cross sections along major north-south gravity profiles.

The procedure is to locate the refraction station on the free-air gravity anomaly map and determine the approximate gravity anomaly value at that point. It is assumed that the structural section, as defined by seismic refraction, remains unchanged along a line of constant free-air gravity value in a region in which the change in age, as indicated by the magnetic anomalies, is small. Where this contour crosses a major north-south gravity profile, the structure is defined. The velocity-density curves of Ludwig, Nafe and Drake (1968) provide a means of converting reported longitudinal wave velocities to densities required for gravity modeling.

A two-dimensional technique (Talwani, 1959) enabled computation of the total vertical attraction of the section assuming infinite horizontal layers and a compensation depth of 30 km. Water depth and sediment thickness at the transposed site were determined from

precision depth recordings and seismic reflection records obtained with a Bolt (40 cubic inch) air-gun system taken simultaneously with the gravity measurements. The transposed station, assumed to have the same total vertical attraction as the original refraction station, was adjusted for the slightly different water depth and sediment thicknesses, giving a consistent structural section along the gravity contour.

Station 21 from Phillips (1964) Gulf of California study, located approximately 100 km from the north end of profile 8 and adjusted as described above, provided the structural control for the north end of the profile (Figure 4). Assuming a spreading half-rate of 3.0 cm/yr, the age of the crust in this area is approximately 8.0 million years. Profile 8, situated approximately midway between the spreading ridges, lies along oceanic crust whose age does not change appreciably along the length of the profile. Since there is no refraction data available south of the Rivera fracture zone, the assumption was made that the oceanic structure in this area remains constant for a given age in undisturbed areas. With this assumption, definition of the south end of profile 8 was also possible.

By adjusting layer thickness so that the computed anomaly best fits the observed, the deep structure of the fracture zone can be inferred across areas where there is no refraction control. Extension of section ends by 5000 km reduced the errors caused by edge

effects. The underlying assumption of two-dimensionality is open to question, but due to the observed linearity of fracture zones, it is a reasonable assumption.

In a similar manner, Station 2 of Shor and Fisher's study of the Middle America trench defined the structure on the north end of profile 11. The 8 million year old section, modified to fit the observed water depth and sediment thickness so that the total vertical attraction was consistent with the free-air anomaly, provided structural control for the south end of profile 11.

No refraction control exists for profile 4, which extends from 2-4 million year old crust in the north to 12-14 million year old crust in the south. Again, the modified 8 million year old section provided the best estimate for layer thickness for the north and south ends of profile 4.

Table 1 shows the control sections derived in the manner shown above, using densities of 1.03, 2.00, 2.61, 2.84 and 3.21 gr/cm^3, for sea water, sediment, layer II, layer III and mantle, respectively. A mantle density of 3.21 gr/cm^3 is slightly lower than densities normally associated with mantle material; but the age of the lithosphere in this area is young enough (less than 14 million years) so that this density is acceptable.

Table 1. Control sections for gravity profiles

Profile	Water Depth (km)	Sediment Thickness (km)	Layer II Thickness (km)	Layer III Thickness (km)	Depth To mantle (km)
4 North	2.9	0.0	1.21	7.07	11.12
4 South	3.5	0.0	1.21	3.47	8.18
8 North	3.1	0.48	1.21	4.33	9.12
8 South	3.5	0.2	1.1	3.3	8.1
11 North	4.8	0.44	.6	7.86	13.7
11 South	3.1	0.0	1.0	6.4	10.5

Structural Profile 4

Profile 4 is the westernmost of the structural sections. It crosses the Rivera fracture zone just east of the East Pacific Rise. It is in this area that the presence of the fracture zone has the greatest topographic relief. In crossing from the south fracture zone ridge to the central trough, a distance of 8 km, the total relief encountered is over 3 km. This relief is partially reflected in the free-air gravity anomaly which drops from a +35 mgals over the south ridge to -110 mgals over the central trough.

The structural section as inferred from the gravity anomaly indicates that the central trough of the fracture zone is underlain by a corresponding trough in the mantle (Figure 6). The normal depth to

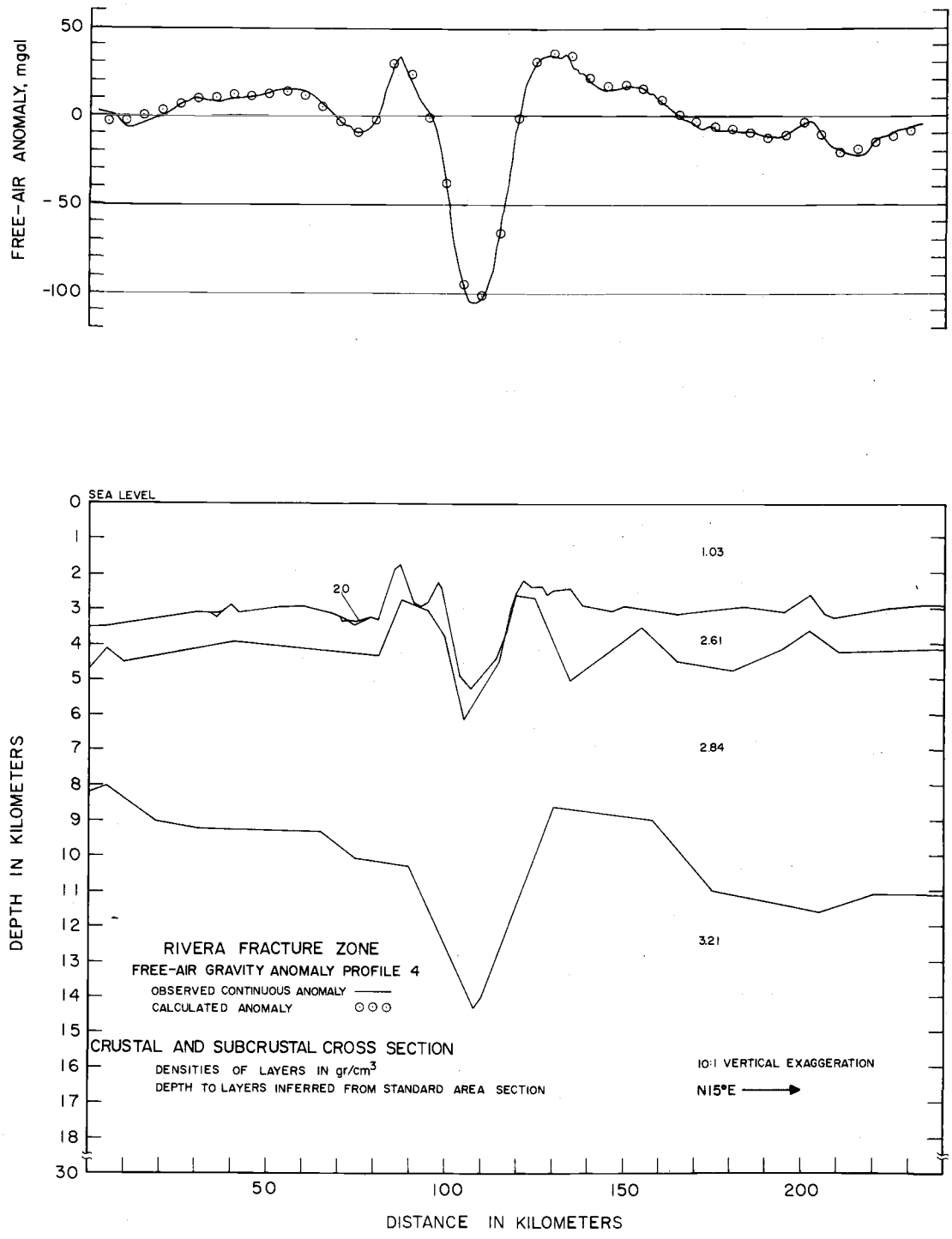

Figure 6. Rivera fracture zone crustal and subcrustal cross section 4.

the top of the mantle in this area is nearly 9 km, but beneath the fracture zone walls, the crust becomes thicker. It reaches a maximum thickness of 8 km directly beneath the central bathymetric trough. This crustal root may also represent altered and fractured upper mantle material.

The fracture zone ridges and troughs also reflect lateral as well as vertical changes in density. The 2.61 gr/cm^3 layer normally associated with oceanic layer II appears to pinch out as a continuous unit in the ridge walls of the fracture zone. The south side of the central trough is composed of 2.61 gr/cm^3 density material which increases to a maximum thickness of 1 km directly under the trough axis and then pinches out in the north wall of the trough. Although this density is associated with layer II outside the fracture zone, in this area it is probably indicative of brecciated and hydrothermally altered basaltic materials or possibly light intrusives. The north wall of the trough is an area of exposed 2.84 gr/cm^3 material, normally indicative of layer II material.

Structural Profile 8

Profile 8 crosses the fracture zone near the termination of the prominent fracture zone topography. Maximum relief in this instance is 2 km vertically in a 5 km traverse. Again, the most predominant feature in the structural section constrained by gravity data is the

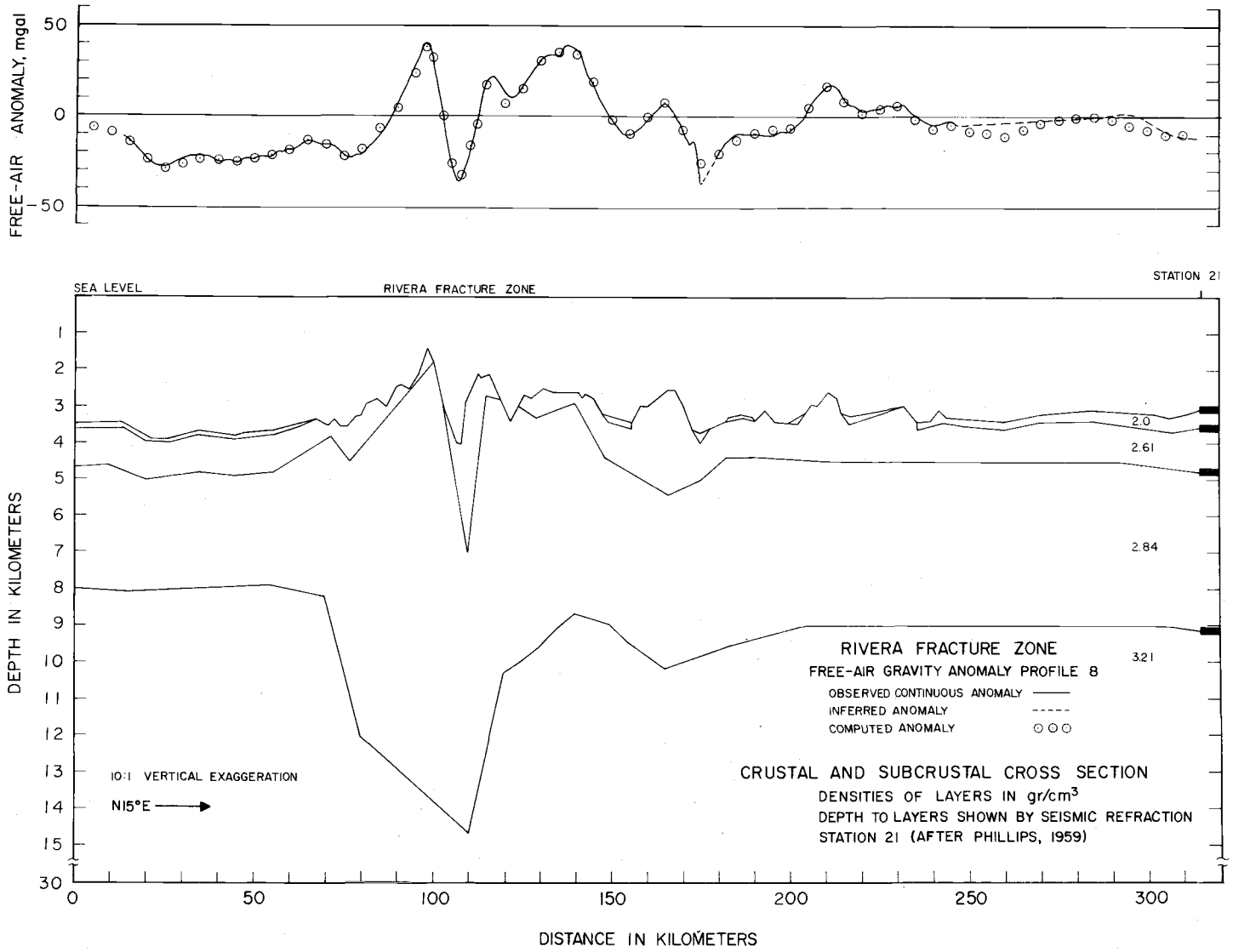

Figure 7. Rivera fracture zone crustal and subcrustal cross section 8.

presence of a deep crustal root beneath the central bathymetric trough (Figure 7). The top of the mantle, with a mean density of 3.21 gr/cm^3, and with a mean depth of 8.5 km, drops to 14 km beneath the trough axis. As in profile 4, the 2.61 gr/cm^3 layer appears to terminate as a continuous unit in the ridge systems which form the walls of the fracture zone. In this case, however, the south trough wall is the zone in which 2.84 gr/cm^3 layer III material is exposed. The north wall is composed of thick 2.61 gr/cm^3 material which reaches a maximum thickness of 3 km directly beneath the trough axis.

Structural Profile 11

Profile 11 lies across the easternmost portion of the fracture zone. This is the area where no apparent bathymetric trace of the fracture zone exists and where earthquake focal mechanisms and epicenters indicate fracturing occurs over a broad zone and in a slightly different direction than in the western portion.

The structural section shows two areas of thickened layer II material directly underlain by a crust-mantle interface which increases in depth from 9 km to nearly 11 km (Figure 8). These two areas are separated by 70 km along the profile. The southernmost zone lies along a line of projection of the western fracture zone topography. The northernmost anomalous zone lies along the east-west striking low lying ridge systems of the eastern Rivera fracture zone area as rep-

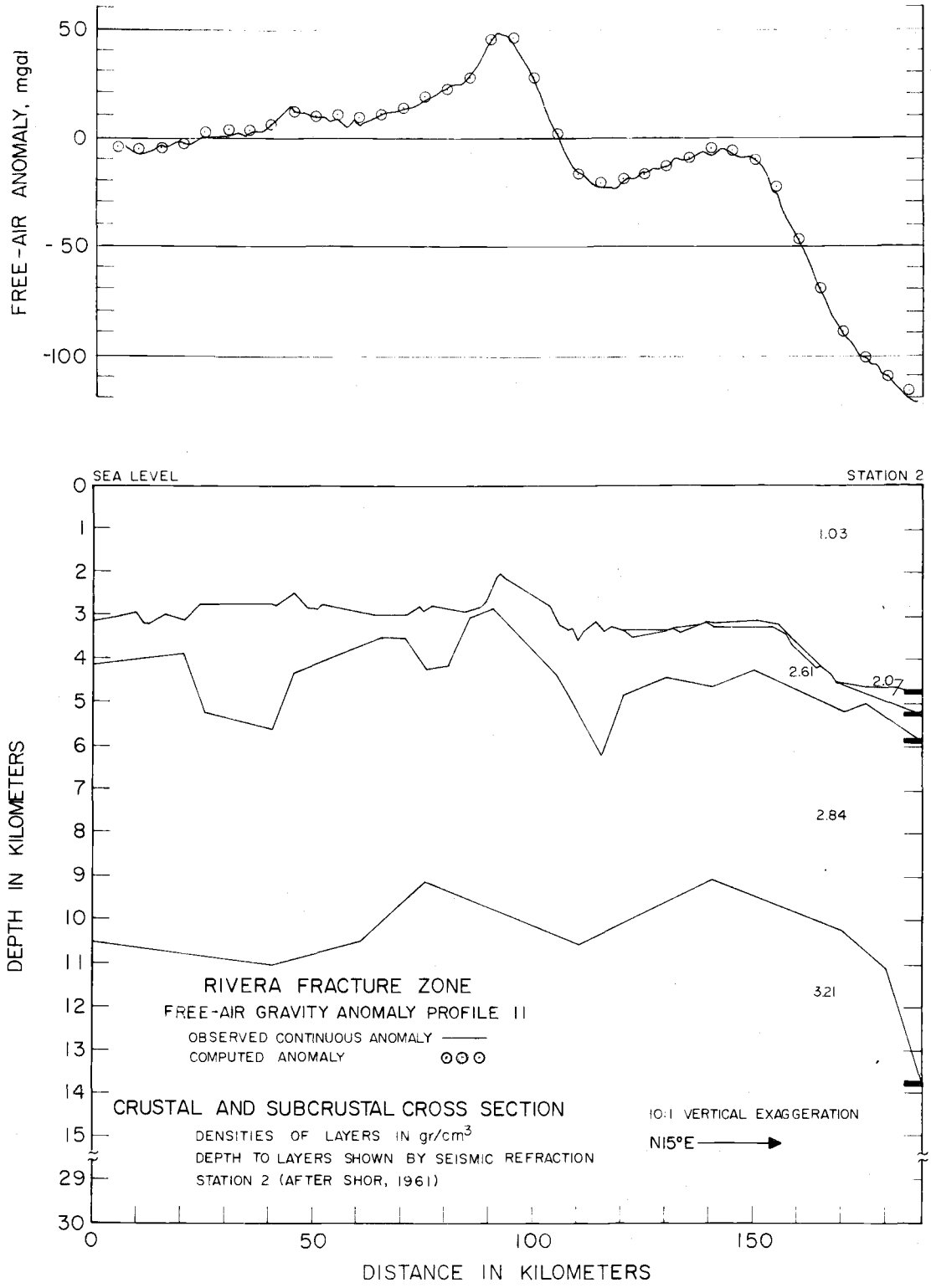

Figure 8. Rivera fracture zone crustal and subcrustal cross section 11.

resented by the 2800 meter contour in Figure 1. It reflects the same general orientation as the easternmost focal mechanism.

General Structure

In general, where topography and a relatively narrow zone of lateral shear motion indicate the presence of a fracture zone, a trough in the mantle underlies the central fracture zone trough. The width of the crustal root is approximately equal to the width of the area of uplift across the fracture zone; i.e., approximately 30 to 40 km. The thickness of the crustal root is from 4 to 5 km.

Layer II of the upper crust appears to terminate in the walls of the fracture zone. The central trough, consists partly of 2.61 gr/cm^3 material, probably indicative of brecciated and altered volcanic material, and partly of heavier material of density 2.84 gr/cm^3. This density is indicative of basic layer III materials such as gabbros or amphibolites. Immediately beneath the floor of the central trough is a narrow root of 2.61 gr/cm^3 material which extends to depths of 3 km below the ocean floor. Again, this low density root is probably indicative of intense fault brecciation and hydrothermal alteration. The nature and origin of this rock cannot be established from the data.

In the eastern portion of the fracture zone, where there is no distinct bathymetry and where fracturing appears to be more diffuse, the crust and mantle exhibit several locally anomalous zones. In

two widely separated areas, the 2.61 gr/cm^3 layer increases in thickness from 1 to 3 km across a 10 to 20 km wide area. Beneath these zones, the crust-mantle interface also gradually deepens by 1 to 2 km, but does so over a wider 50 to 60 km area.

Considering the seismic evidence and local tectonic setting, these anomalous areas may indicate sites of lateral faulting associated with the Rivera fracture zone. Fracturing evidently occurs over a much broader zone. It appears that the result of spacing a constant amount of fracturing or total differential shear motion over a larger area is to alter wider areas of crust and mantle to a lesser extent.

Magnetics

Modeling Techniques

Slab models were constructed for profiles 4 and 8 directly from depth corrected digitized bathymetry records. Spatial frequency of the field data is approximately 2.0 points per km, but varies with the amount of relief encountered; i.e., higher frequency over the fracture zone. The magnetic data was sampled at a frequency of 1.25 points per km and a theoretical anomaly is calculated at 1.0 points per km, the uncertainty therefore being slightly greater at the higher frequencies.

The purpose of the magnetic modeling is not to infer layer thicknesses or intensity of magnetization by fitting the observed curve exactly, but to use standard accepted values for thickness and intensity of magnetic sources along with topography in order to fit the general shape and amplitude of the observed anomalies using the simplest possible model.

One important source of error in both gravity and magnetic modeling lies in using unmigrated bathymetry for the surface of source bodies. Many of the first returns over steeper portions are portions of reflection hyperbolas and not true bottom. This severely limits the steepest slope which can be seen. In general, the maximum slope which can be accurately recorded is 0.5 x the cone angle of the P.D.R. or in this case 30°. This means that a 90° fault scarp in the fracture zone appears as a moderately sloping face in the models.

Theoretical anomalies were calculated using a two-dimensional modeling technique of Talwani and Heirtzler (1964). Again, the assumption of two-dimensionality on the fracture zone is a good approximation of the real configuration.

Description of Observed Magnetic Profiles

Figure 10 shows the bathymetry and observed magnetic anomaly over profiles 4 and 8. Both show anomalies of up to 500 gammas, several of these seem to correlate with topographic features while others

do not. At this point, it is impossible to even guess at the source of the anomalies without including topographic effects.

At first glance, the observed magnetic data do show a large anomaly in the area of the fracture zone trough. However, a careful look at the magnetic and bathymetric profiles will show that the large positive anomaly does not appear to be associated with the fracture zone trough, but instead with the prominant walls of the fracture zone.

It is likely that cursory examinations of data at high vertical exaggeration has been the source of some misleading descriptions of the magnetic signature of fracture zones.

Induced Magnetic Profiles

There is no evidence for re-orientation of the crust in the Rivera fracture zone area since its formation, consequently, it is virtually impossible to distinguish between a magnetic anomaly caused by induced magnetization and normally polarized remnant magnetization. However, the differences between an anomaly caused by induced magnetization and an anomaly caused by reversely polarized remnant magnetization are great and it is possible to distinguish between them with some degree of certainty.

The first step in the magnetic modeling was to calculate the anomaly produced by induced magnetization from a 1.0 km thick layer which follows the topography and has an induced susceptibility of

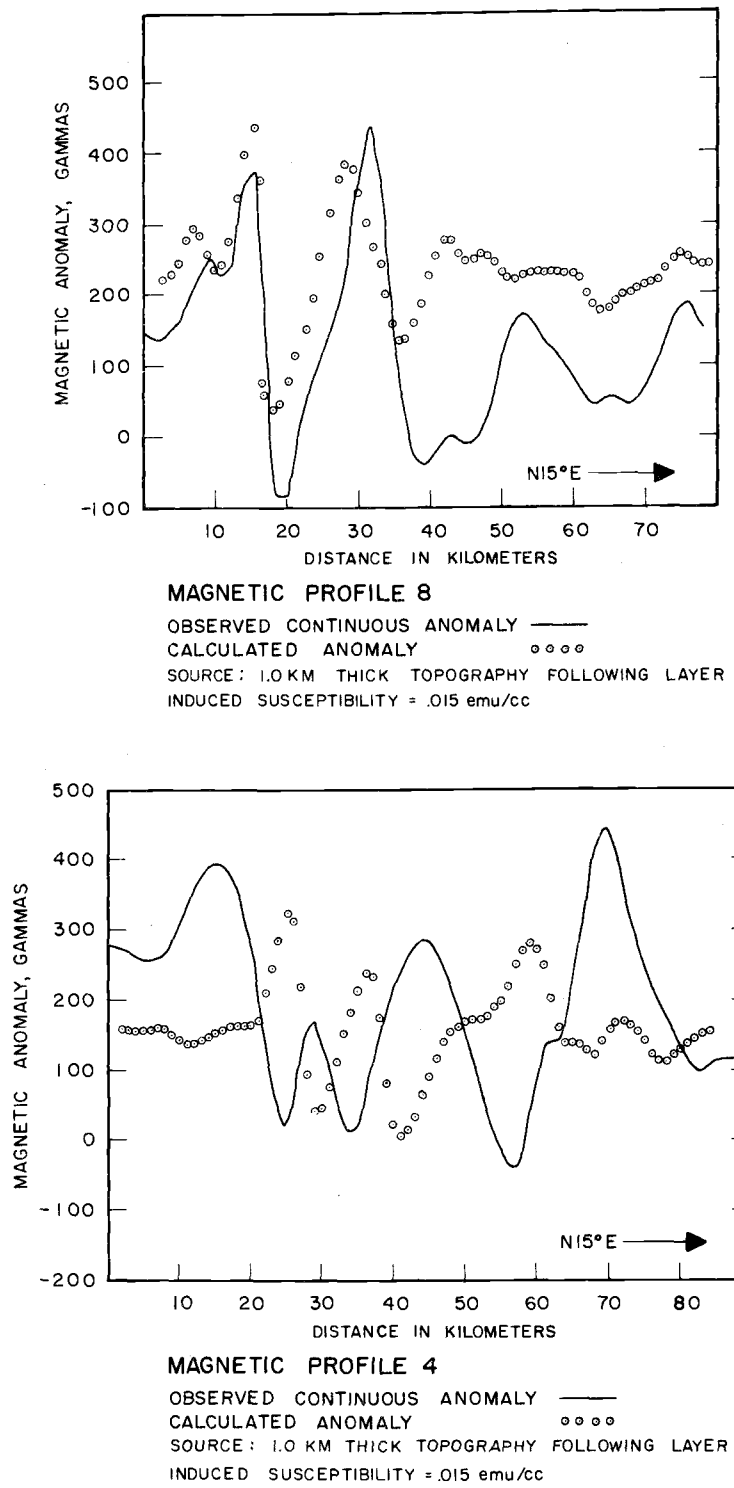

Figure 9. Observed and theoretical magnetic anomalies over profiles 4 and 8. Models assume source bodies with induced magnetization.

.015 emu/cm^3. This susceptibility is high for oceanic basalts, but necessary to reproduce the required anomaly amplitudes.

Figure 9 shows the calculated induced field superimposed upon the observed anomalies for profiles 4 and 8. Profile 8 fits the observed anomaly shapes fairly well, but the calculated peak to peak amplitudes are over 100 gammas too low over the fracture zone. However, in profile 4, the theoretical induced anomaly appears to be opposite in sense to the observed anomaly. The simplest source which could possibly produce the observed anomaly for profile 4 is a reversely polarized remnant source.

Contrary to recent investigations (Cochran, 1973), this seems to rule out the possibility of explaining the Rivera fracture zone anomalies by induced magnetic source bodies.

Remnant Magnetic Models

Profiles 4 and 8 were remodeled using remnant magnetic fields in a 0.5 km thick source layer following the topography and having an intensity of remnant magnetization of .022 emu/cm^3. This is a more reasonable value for magnetization of oceanic basalts than was the value of induced susceptibility required to produce compatible theoretical and observed anomaly amplitudes.

Since the gravity data suggested that the fracture zone is the site of brecciation and hydrothermal alterations due to large scale lateral

faulting, it is difficult to envision an unbroken magnetized layer lying beneath the fracture zone. Even if this was originally the case, one would expect the intensity of the remnant magnetization of layer II basalts to be essentially zero in the central fracture zone area. Matthews et al. (1965) noted the expunging of magnetic anomalies associated with the Carlsberg Ridge in a wide area near a fracture zone. Dredge hauls from the walls of the fracture zones produced brecciated basalts which showed varying degrees of hydrothermal alteration. Accordingly, profiles 4 and 8 were modeled so that the 0.5 km thick layer was discontinuous across the fracture zone trough so as to render the center 5-8 km of the fracture zone nonmagnetic.

Figure 10 shows the remnant models with the calculated and observed anomals. Although the fit in profile 8 does not improve greatly, the observed and calculated anomaly amplitudes more closely match over the central fracture zone area. The effect of introducing this nonmagnetic zone effectively increases the central anomaly amplitudes. The fit on profile 4 improves drastically. The 400 gamma anomaly near the north end of the profile is apparently produced by a change in polarity between the fracture zone axis and the end of the profile. This is entirely possible since the traverses were up to 15^{o} off perpendicular to the exact strike of the fracture zone and since the polarity bands are not necessarily linear features. The anomaly on the south end of the profile could be modeled in any of several differ-

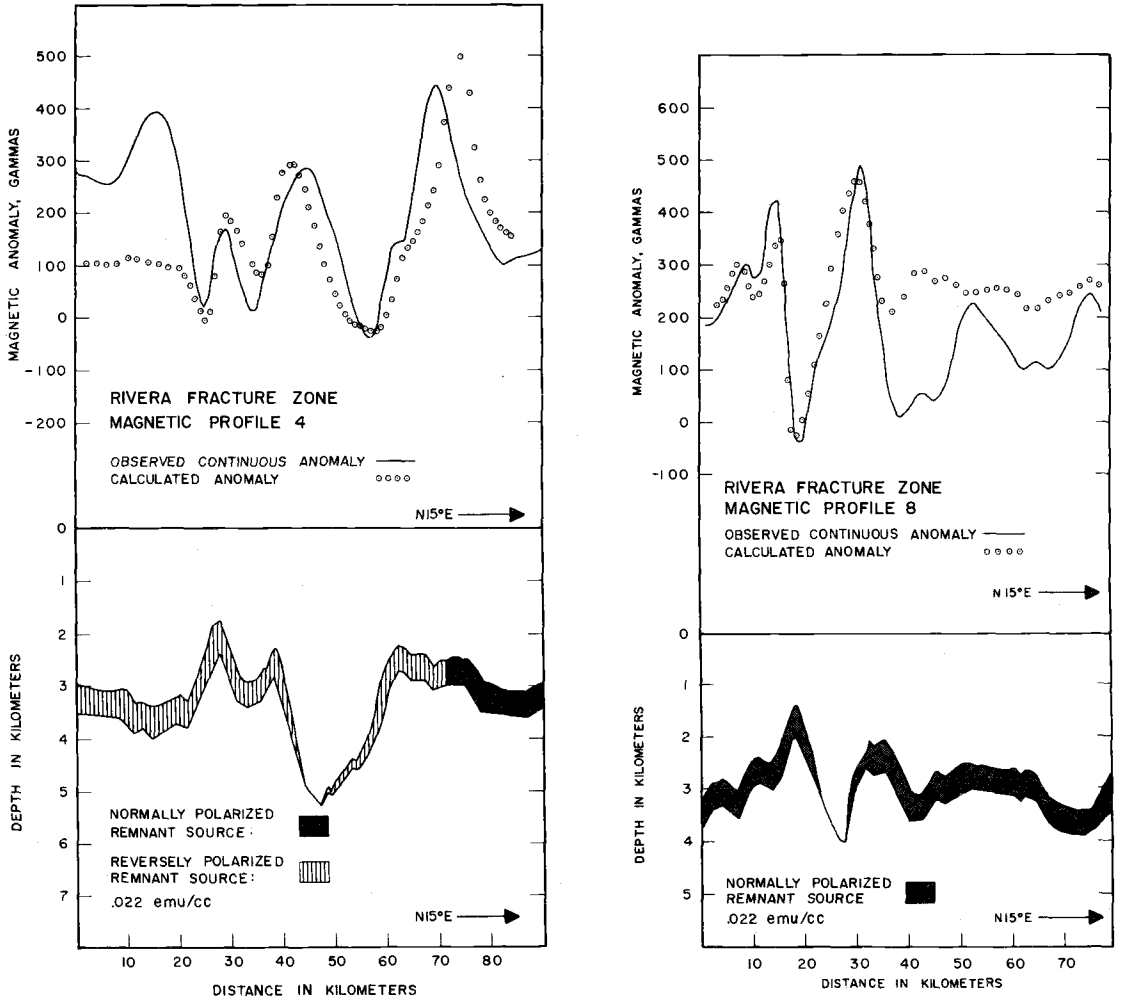

Figure 10. Observed and theoretical magnetic anomalies over profiles 4 and 8. Models assume source bodies with remnant magnetization.

ent ways, but since there is no gravity or structural data which might indicate its source, no effort was made to model it. The anomaly is over 35 km from the fracture zone, and it is unlikely that the two could be directly related.

It is possible that many different sources, dependent upon local tectonics and the particular fracture zone, could cause the observed fracture zone anomalies. However, the anomalies associated with the Rivera fracture zone appear to be caused by layer II basalts which are terminated in the fracture zone walls. Topographic effects complicate the observed magnetic anomalies making their interpretation possible only after this effect was taken into account.

To account for the Rivera fracture zone magnetic anomalies with induced magnetization, or bodies sub-parallel to the fracture would require much more complicated models.

Combined Magnetic and Gravity Models

The gravity and magnetic models, generated independently, yield basically the same structural results for the upper oceanic crust. The fact that no intrusive bodies are necessary to account for the observed magnetic anomalies supports the gravity models which introduced no additional layers than were previously indicated by the refraction data available for the area.

The configuration of the magnetic layer and the 2.61 gr/cm^3 layer in the fracture zone trough at first glance do not appear consistent. Recently, however, investigators in magnetics have tended to attribute much of the remnant magnetic anomaly field to a very thin layer of intensely magnetized pillow basalts on the sea floor (Cox, et al., 1972). These small scale features may not necessarily show up in a gravity model. Conversely, the presence of the 2.61 gr/cm^3 layer in the gravity model does not necessarily imply a magnetic source. The layer may have lost much of its magnetization, or may consist of non-magnetic material. However, the essential conclusion is that the two independent non-unique solutions lead to the same general conclusions concerning the structure of the Rivera fracture zone.

Any structural model for a fracture zone should be examined in the light of the existing petrological data. Although this adds no further structural information, it is useful in estimating the validity of some models generated from potential field data. In general, the structural model presented for the Rivera fracture zone is compatible with present day petrological models. The appearance of both 2.61 and 2.84 gr/cm^3 layers in the trough walls may account for the presence of both basalts and basic rocks and their associated alteration products obtained in dredge hauls from fracture scarps. Although large amounts of altered peridotites have not been dredged

from Pacific fracture zones, the presence of an altered mantle root beneath the Rivera fracture zone would make the central trough a very likely place to find altered basic and ultrabasic rock such as serpentines.

TECTONICS OF A FRACTURE ZONE AND AN ALTERNATE THEORY FOR THE ORIGIN OF FRACTURE ZONE TOPOGRAPHY

Presently, only the modified model of Sleep and Biehler (1970) successfully accounts for some aspects of fracture zone topography. The limitations of this type of theory have already been examined, but perhaps the major argument in favor of a more general theory is the profusion of fracture zones existing in all types of tectonic environments and all exhibiting generally similar topography. The topographic variability of fracture zones from ocean to ocean is less than the variability of the mid-ocean ridge systems with which they are associated. These facts lead one to conclude that tectonic forces independent of the rise systems contribute to the building of fracture zone topography.

A fracture zone is a transition region across which lateral shear motion in thick lithospheric plates occurs. This transition zone must extend to at least the depth past which elastic processes are no longer the predominant mode of deformation. This depth is not well defined in the oceanic crust, but earthquake hypocenters have been located at least as deep as 15 km along fracture zones (e.g., Tobin and Sykes, 1968).

Crustal cross sections derived from refraction controlled gravity and magnetic data presented in preceding sections suggest that fracturing occurs across a 30 km wide area enclosing the fracture zone

ridges and trough. An intensely fractured and brecciated zone from 5 to 7 km wide probably exists in the central trough of the fracture zone. Below the floor of the fracture zone, is a relatively narrow low density zone underlain by an anomalously deep and narrow mantle trough.

Constant faulting and brecciation of the crust and upper mantle material in the fracture zone appear to occur to depths of at least 10 km beneath the ocean floor. The resulting increase in permeability associated with fracturing of crust and mantle rocks could provide an environment in which water, in some form, might be expected to exist at great depths. Hydrothermal currents as deep as 750 meters in faulted basaltic areas are well documented (Bodvarsson, 1972). Hart (1973) postulates the existence of water from 3-5 km in order to account for alteration of basalts on mid-ocean ridge flanks, and Lister (1972) proposes the existence of water at depths of up to 10 km beneath Juan de Fuca Ridge.

If this is indeed the case, then it is not unlikely that a fracture zone may also be the site of deep water penetration. The immediate result of water injection is the alteration of crustal and mantle material beneath the fracture. Alteration products of the upper oceanic crust vary considerably with the initial chemical and mineral composition of the host rock, the thermal regime, and the time available for alteration (Hart, 1970, 1973). Such information for the upper crust cannot be

ascertained from the geophysical data presented in this text. However, the presence of an anomalous mantle root and its associated density contrast may indicate something more definite concerning subcrustal alterations.

One immediate result of hydrothermal alteration is a reduction of density in the altered material. The question of whether serpentinization of periodotite results in a volume expansion of the altered material is the subject of some controversy. If the chemical system is not restricted exclusively to water introduction, then the formation of serpentine is possible without a corresponding volume increase (Thayer, 1966). However, field studies by Coleman and Keith (1970) on Burro Mountain, California, indicate that serpentinization of peridotite can proceed under isochemical conditions (except for the injection of water). They state that "a completely serpentinized dunite ($\sim$ 100 wt per cent olivine) with a final brucite/serpentine ratio of 0.21 will have a volume increase of 48 percent." They conclude that 32 percent serpentinization occurred in their study area with a 14 percent volume increase. This process probably proceeded in stages with moderate volume increases accommodated by faulting which allowed vertical and horizontal movement.

If it is assumed that the crust-mantle interface in the Rivera fracture zone area was originally at a depth of 8-9 km, then approximately 150 cubic km of mantle material was altered beneath each

1 km length of the fracture. The gravity models indicate a density decrease from 3.21 to 2.84 gr/cm^3, which corresponds to a 14 percent volume increase. The result of this volume expansion will be to cause localized uplift in the 4-5 km thick rigid plates overlying the expansion zone.

The total amount of expansion and the time required for that expansion depends upon the vertical and horizontal extent of faulting and the rate and extent of alteration. Regional tectonics control the extent of horizontal faulting, and material parmeters control the depth of faulting. The gravity sections support this by indicating no appreciable change in the volume of altered material with age along the fracture zone. This means that the controlling factor in rate and extent of expansion is the degree and rate of alteration. Rates for this process at depth are largely unknown, but the appearance of fracture zone topography in new crust formed at the ridge-fracture intersection requires the rate of expansion to be large when compared to the rate of horizontal movement. There is also no clear evidence for large amounts of continued uplift with age on the fracture zone, which means that most of the hydrothermal alteration and accompanied expansion occurred in a relatively short time.

Figure 11A depicts faulting in oceanic crust and mantle due to transverse motions in lithospheric plates. The overall permeability of a fault brecciated section increases, allowing the penetration of

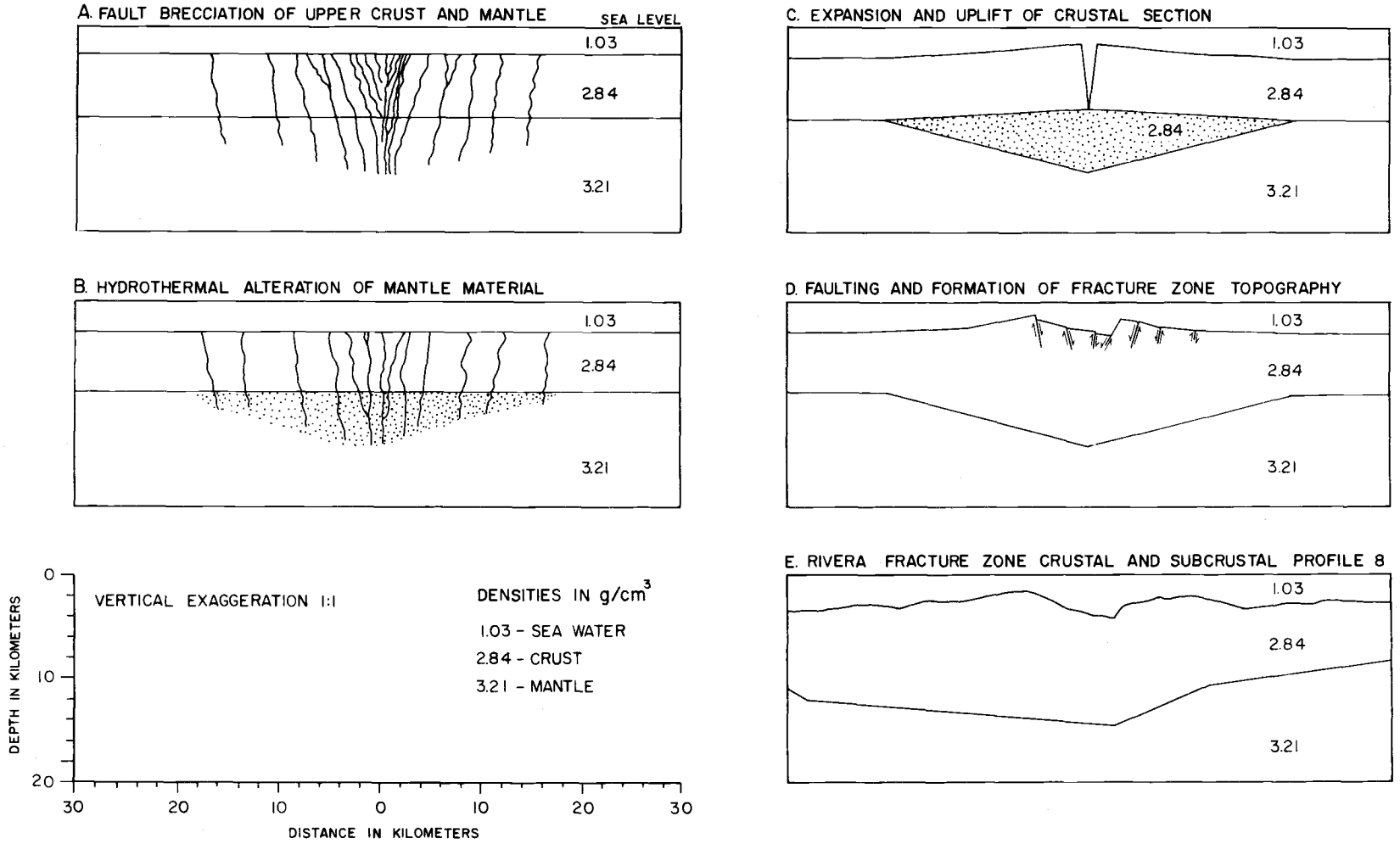

Figure 11. Evolution of fracture zone topography and Rivera fracture zone profile 8.

water through the crust and into the upper mantle. Water, in contact with mantle materials, causes the hydrothermal alteration of the host rock (Figure 11B). Alteration of mantle material brings about a reduction in density and expansion in the altered volume; which in turn causes uplift in the crustal sections overlying the altered material. Uplift across two structurally independent plates will result in crustal dilation, and the generation of a void area between the two plates (Figure 11C). Faulting, accompaning the uplift and the structural instability in the regions nearest the void, will result in the formation of a central valley bordered by raised parallel ridges (Figure 11D). Less extensive uplift and faulting on the fracture zone flanks produce sub-parallel valleys and ridges. The processes of alteration, uplift and faulting are contemporaneous. This hypothetical topography is compared to the Rivera fracture zone profile 8 with no vertical exaggeration (Figure 11E).

Where a well defined fracture zone intersects a spreading ridge, this topography would immediately begin forming. It would also occur along previously unaltered oceanic crust subjected to the presence of fracture zone faulting. This may help explain the troubling presence of fracture zone topography along oceanic crust which was formed far from a fracture-spreading ridge intersection. Where faulting occurs across a broader area, the extent of alteration is less, and distinct fracture zone topography does not form.

Local uplift and subsidence across fracture zones produces observable vertical faulting. This is apparent in profiles across the Ascension fracture zone in the equatorial Atlantic Ocean which shows vertically offset sedimentary sections (van Andel, et al., 1973).

This simple model is not intended to account for all aspects of fracture zone topography. In particular, the time required to create fracture zone topography in this manner is largely unknown. Because of the appearance of deep valleys immediately at the rift-fracture intersections it is probable that at this location, the Sleep and Biehler (1971) model may be more applicable. It is also unclear as to how this model might be adapted to fit the postulated "leaky" fracture zones of the central Atlantic.

However, this simple model for the origin of fracture zone topography does fit the existing data for the Rivera fracture zone and accounts for the presence of fracture zone topography along sections of oceanic crust where previously existing theories do not apply. More importantly, it provides a common mechanism for producing distinct topography on fracture zones which may lie in entirely different geographical and tectonic settings.

BIBLIOGRAPHY

Aumento, F. and H. Loubat. 1971. The Mid-Atlantic Ridge near 45°N, XVI serpentinized ultramatic intrusions. Canadian Journal of Earth Sciences 8:631-663.

Bodvarrson, G. and R. P. Lowell. 1972. Ocean floor heat flow and circulation of interstitial waters. Journal of Geophysical Research 77:4472-4475.

Bonatti, E., J. Honnorez and G. Ferrara. 1970. Equatorial Mid-Atlantic Ridge: petrological and Sr isotope evidence for an alpine-type rock assemblage. Earth and Planetary Science Letters 9:247-256.

Cochran, J. R. 1973. Gravity and magnetic investigations in the Guiana Basin, western equatorial Atlantic. Journal of Geophysical Research. (In press).

Coleman, R. G. and T. E. Keith. 1970. A chemical study of serpentinization-Burro Mountain, California. Journal of Petrology 12:311-328.

Cox, A., B. J. Blakely and J. D. Phillips. 1972. A two-layer model for magnetic anomalies. Transactions of the American Geophysical Union, 53:947.

Dehlinger, P., R. W. Couch and M. Gemperle. 1967. Gravity and structure of the eastern part of the Mendocino escarpment. Journal of Geophysical Research 72:1233-1247.

Hart, R. A. 1970. Chemical exchange between seawater and deep ocean basalts. Earth and Planetary Science Letters 9:269-279.

_____. 1973. A model for chemical exchange in the basalt-seawater system of oceanic layer II. Canadian Journal of Earth Sciences 10:799-816.

Isacks, B., J. Oliver and L. R. Sykes. 1968. Seismology and the new global tectonics. Journal of Geophysical Research 73:5855-5900.

Larson, R. L. 1972. Bathymetry, magnetic anomalies and plate tectonic history of the mouth of the Gulf of California. Geological Society of America Bulletin 83:3345-3360.

Lister, C. R. B. 1972. On the thermal balance of a mid-ocean ridge. Geophysical Journal of the Royal Astronomical Society 26:515-535.

Ludwig, W. J., J. E. Nafe and C. L. Drake. 1971. Seismic refraction. In: The Sea, Volume 4, Part I, ed. by Arthur E. Maxwell, New York, Wiley, p. 53-84.

Matthews, D. H., F. J. Vine and J. R. Cann. 1965. Geology of an area of the Carlsberg Ridge, Indian Ocean. Geological Society of America Bulletin 76:675-682.

Melson, W. G. and G. Thompson. 1970. Layered basic complex in oceanic crust. Science 168:817-820.

_____. 1971. Petrology of a transform fault zone and adjacent ridge segments. Philosophical transactions of the Royal Society of London. 268:423-441.

Menard, H. W. and R. S. Dietz. 1952. Mendocino submarine escarpment. Journal of Geology 60:266-278.

Menard, H. W. 1964. Marine geology of the Pacific. New York, McGraw-Hill. 271 p.

Menard, H. W. and T. Atwater. 1969. Origin of fracture zone topography. Nature 222:1037-1040.

Molnar, P. 1973. Fault plane solutions of earthquakes and direction of motion in the Gulf of California and on the Rivera fracture zone. Geological Society of America Bulletin 84:1651-1658.

Morgan, W. J. 1968. Rises, trenches, great faults and crustal blocks. Journal of Geophysical Research 73:1959-1982.

_____. 1969. Magnetic survey of the Juan de Fuca Ridge. (Abstract) Transactions of the American Geophysical Union 50:185.

Phillips, R. P. 1964. Seismic refraction studies in the Gulf of California. In: Marine Geology of the Gulf of California, p. 90-121. (A symposium of the American Association of Petroleum Geologists. Memoir 3).

Rea, D. K. 1972. Magnetic anomalies along fracture zones. Nature Physical Science 236:58-59.

Shor, G. G., Jr. and R. L. Fisher. 1961. Middle America Trench: seismic-refraction studies. Geological Society of America Bulletin 72:721-730.

Sleep, N. H. 1969. Sensitivity of heat flow and gravity to the mechanism of sea-floor spreading. Journal of Geophysical Research 74:542-549.

Sleep, N. H. and S. Biehler. 1970. Topography and tectonics at the intersections of fracture zones with central rifts. Journal of Geophysical Research 75:2748-2752.

Sykes, L. R. 1967. Mechanism of earthquakes and nature of faulting on the mid-ocean ridges. Journal of Geophysical Research 72:2131-2154.

Sykes, L. R. 1968. Seismological evidence for transform faults, sea-floor spreading, and continental drift. In: The History of the Earth's Crust, ed. by R. A. Phinney, Princeton, Princeton University: 120-150.

Talwani, M., J. L. Worzel and M. Landisman. 1959. Rapid gravity computations for two-dimensional bodies with application to the Mendocino submarine fracture zone. Journal of Geophysical Research 64:49-59.

Talwani, M., and J. P. Heirtzler. 1964. Computation of magnetic anomalies caused by two-dimensional structures of arbitrary shape. In: Computers in the Mineral Industries (6.A. Parks, ed.) Stanford University Publications. Vol. IX. No. 1, p. 464.

Thayer, T. P. 1966. Serpentinization considered as a constant volume metasomatic process. The American Mineralogist 51:685-710.

Thompson, G. and W. G. Melson. 1972. The petrology of oceanic crust across fracture zones in the Atlantic Ocean: evidence of a new kind of sea-floor spreading. The Journal of Geology 80:526-538.

Tobin, D. G. and L. R. Sykes. 1968. Seismicity and tectonics of the northeast Pacific Ocean. Journal of Geophysical Research 73:3821-3845.

van Andel, Tj.H., J. D. Phillips and R. P. von Herzen. 1968. Rifting origin for the Vema fracture in the North Atlantic. Earth and Planetary Science Letters 5:296-300.

van Andel, Tj.H., R. P. von Herzen and J. D. Phillips. 1971. The Vema fracture zone and the tectonics of transverse shear zones in the oceanic crustal plates. Marine Geophysical Researches 1:261-283.

van Andel, Tj.H., D. K. Rea, R. P. von Herzen and H. Hoskins. 1973. Ascension fracture zone, Ascension Island, and the Mid-Atlantic Ridge. Geological Society of America Bulletin 84:1527-1546.

Vogt, P. R., C. N. Anderson and D. R. Bracey. 1971. Mesozoic magnetic anomalies, sea-floor spreading and geomagnetic reversals in the south-western North Atlantic. Journal of Geophysical Research 76: 4796-4823.

Wilson, J. T. 1965. A new class of faults and their bearing on continental drift. Nature 207:343-347.